Research Article

Journal of Environmental Nanotechnology

Structural, Morphological and Optical Properties: CeO_2 Nanoparticles Prepared through the *Azadirachta indica* Leaf Extract by Green Method

S. Parvathy[1*], B. R. Venkatraman[2]

[1]Department of Chemistry, Government Arts College, Salem, TN, India
[2]Department of Chemistry, Periyar E.V.R. College, Tiruchirappalli, TN, India
Received: 10.07.2017 Accepted: 16.08.2017 Published: 30-12-2017
*paruchem70@gmail.com

ABSTRACT

The CeO_2 NPs were derived from *Azadirachta indica* (A.indica) leaf extracts. The X-ray diffraction studies confirmed that synthesized CeO_2 NPs were exhibited the cubic structure. In XPS spectra, the oxidation states of each element were identified for CeO_2 NPs. The Raman active mode was observed at 461cm^{-1}, and this was due to the symmetrical stretching mode of the Ce-8O for CeO_2 NPs. From FESEM and TEM images, the CeO_2 NPs were exhibited a spherical structure. From the EDAX spectra, the elemental compositions were identified. The optical studies were carried out using UV-Vis and Photoluminescence spectra for CeO_2 NPs, respectively.

Keywords: Photosynthesis; CeO_2; Nanoparticles; Optical studies.

1. INTRODUCTION

The CeO_2 nanoparticles could be a technologically potent material with remarkable properties utilized in a variety of applications in Environmental science. The CeO_2 nanoparticles have been used as three-way catalysts (TWC) for exhaust gas treatment from automobiles, oxygen ion conductors in solid oxide fuel cells, polishing agents for the chemical, mechanical planarization (CMP) process, gate oxides in metal oxide semiconductor devices, and ultraviolet (UV) blocking materials in UV shielding, respectively (Zhang *et al*. 2003; Si *et al*. 2005; Yu *et al*. 2005; Wang *et al*. 2003; Miki *et al*. 1990; Tsunekawa *et al*. 2000).

The synthesized CeO_2 NPs were prepared by physical and chemical methods such as hydrothermal, flame spray pyrolysis, sonochemical, microwave, sol-gel, and co-precipitation (Zhang *et al*. 2003; Hu *et al*. 2007; Wang *et al*. 2002; Liao *et al*. 2001; Czerwinski *et al*. 1997; Yao and Xie, 2007). However, most of the techniques are difficult, time-intense, high priced, and unsafe. Green chemistry approaches the event in photosynthesis of metal and metal oxide NPs. This method offers several benefits like cost-effectiveness, large-scale industrial production, and pharmaceutical applications.

In the present investigation, CeO_2 NPs are prepared through the *Azadirachtaindica* leaf extract. The synthesized nanoparticles are characterization work done by the structural, morphological, and optical CeO_2 NPs.

1.1 Material and Methods

1.1.1 Green synthesis CeO_2 NPs

The 10 g of finely divided leaves of *Azadirachtaindica*was added to 100 mL of double distilled water and boiled at 50-60°C for 10 min. The solution was filtered through Whatmann No. 1 filter paper, and the clear filtrate was collected and which were carried for further usage. Thereafter, add a certain quantity of 0.1M solution of cerium nitrate to 100 mL of *A. indica* leaf extract with constant stirring at 80 °C for 6h. The Initially brown precipitate was formed, and then it becomes a yellowish-brown in color on continuous stirring. Finally, the precipitate was dried at 120 ˚C. The precipitate was annealed at 400 °C for 5h to get spherical NPs.

1.1.2 Characterization techniques

The CeO_2 NPs were characterized by an X-ray diffractometer (model: X'PERT PRO PANalytical). The diffraction patterns were recorded in the range of 20°-80° for the CeO_2 NPs samples, where the monochromatic wavelength of 1.54 Å was used. The XPS measurements were performed with an XPS instrument (Carl Zeiss) equipment. The spectra were at a pressure using an ultra-

high vacuum with Al Kα excitation at 250 W. The samples were analyzed by Field Emission Scanning Electron Microscopy (Carl Zeiss Ultra 55 FESEM) with EDAX (model: Inca). TEM analyses were carried out by the instrument Philips CM 200 model operated at an accelerating voltage of 20-200kv Resolution: 2.4 A°. The FT-IR spectra were recorded in the range of 400-4000 cm^{-1} by using a Perkin-Elmer spectrometer. The absorption spectra of CeO_2NPs were studied in the range between 200 and 800nm by Lambda 35 spectrometers. Photoluminescence spectra were measured using the Cary Eclipse spectrometer.

2. RESULTS & DISCUSSIONS

2.1 Structural Analysis

The X-ray diffraction patterns of CeO_2 NPs derived from A. indica leaf extract are shown in Fig. 1. The standard diffraction peaks show the face-center cubic phase of CeO_2 NPs (JCPDS data Cardno: 34-0394). The lattice constant 'a' values are 5.4108 Å for CeO_2 NPs. The average crystallite sizes are found to be 9.2 nm. The XPS of CeO_2 NPs derived from *A. Indica* leaf extract is shown in Fig. 2. The XPS provides information on the oxidation state of each element in the sample as well as the composition of the surface functionalization of the CeO_2NPs. The XPS results show that the indexed peaks correspond to the C (1s), O (1s), and Ce (3d) for the CeO_2 NPs. The C (1s) signals are most likely due to trace amounts of plant or simply due to the absorption of organic contaminants. The Raman spectra of CeO_2 NPs derived from *A. Indica* leaf extract are shown in Fig. 3. From the Raman spectra, the sharp Raman active mode is observed at 461cm^{-1}. This is due to the symmetrical stretching mode of the Ce-8Ofor CeO_2 NPs. However, this peak is very sensitive to any disorder in the oxygen sub-lattice results, changing in physical and chemical properties (Arumugam *et al*.; 2015).

2.2 Morphological and Elemental Analysis

The surface morphology and elemental composition of CeO_2 NPs derived from *A. Indica* leaf extract are shown in Fig. 4(a-b). The FESEM and TEM image clearly shows the average sizes of the NPs are in 5-6 nm range. The CeO_2 NPs exhibit a spherical structure. From the EDAX spectra (see fig. 4c) CeO_2 NPs, the atomic percentage of Ce, C, and O were found to be 64.03 %, 20.15%, and 15.82%, respectively.

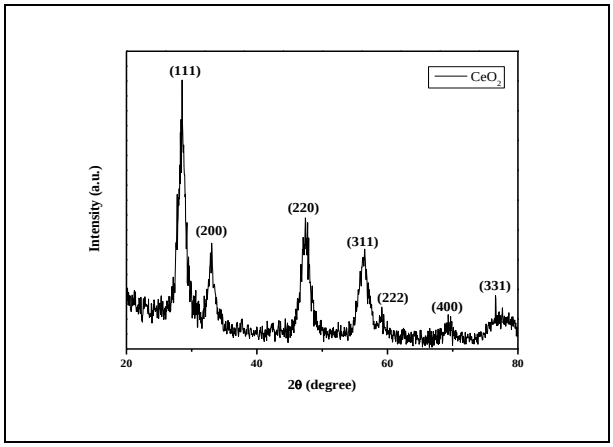

Fig. 1: X-ray diffraction pattern of CeO_2 NPs.

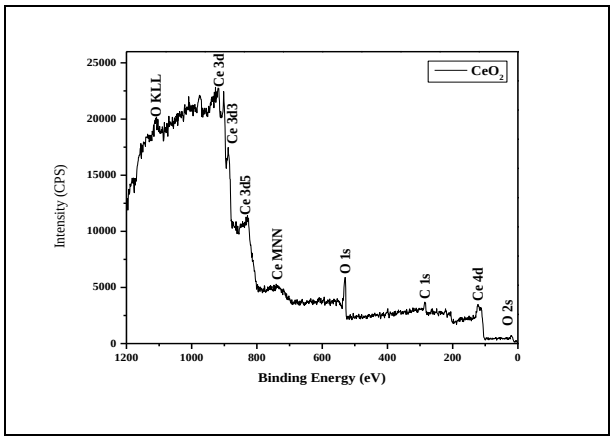

Fig. 2: XPS spectra of CeO_2 NPs.

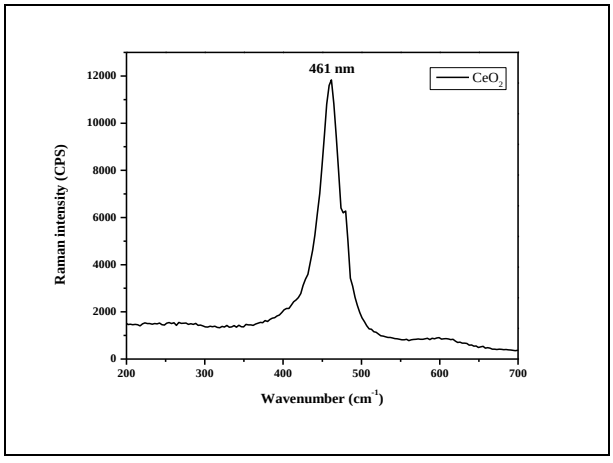

Fig. 3: FT-Raman spectra of CeO_2 NPs.

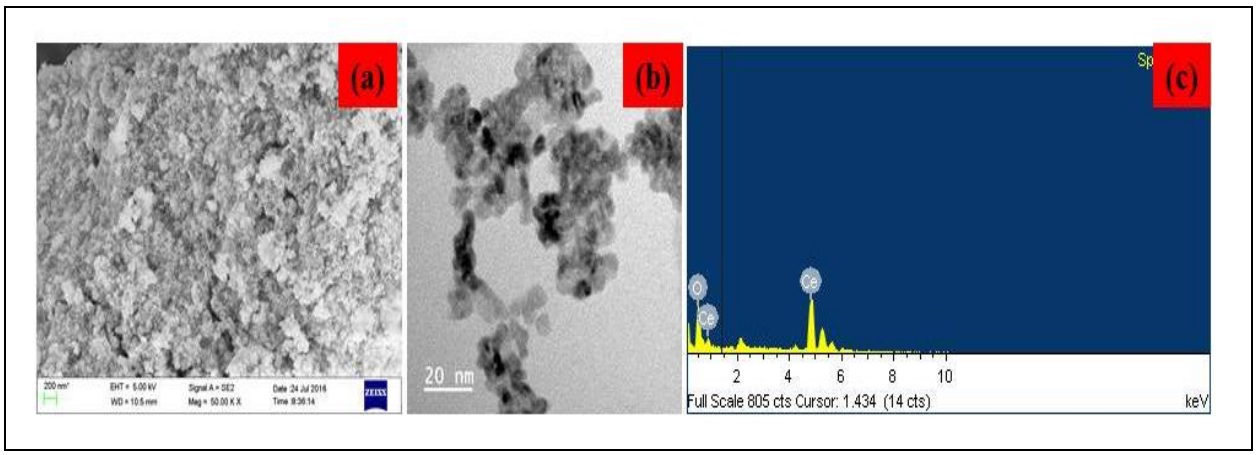

Fig. 4: (a-c) Morphology images of (a) FESEM, (b) TEM and (c) EDAX spectra of CeO_2 NPs.

2.3 Optical Studies

The UV-VIS spectra of CeO_2 NPs derived from *A. indica* leaf extract are shown in Fig. 5. *A. indica* leaf extract consists of phytoconstituents acting as a capping and reducing agent. So, it has reduced to form the CeO_2 NPs. The absorption edge is observed at 314 nm for CeO_2 sample. This can be attributed to the photoexcitation of electrons from the valence band to the conduction band0.

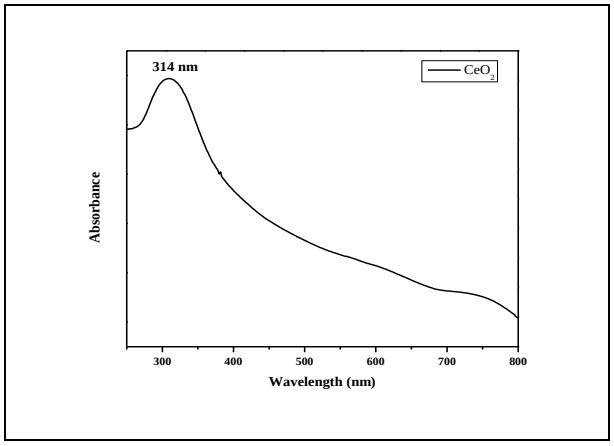

Fig. 5: UV-Vis absorption spectra of CeO_2 NPs.

The photoluminescence spectra of the CeO_2 NPs derived from *A. indica* leaf extract were recorded with the exciting wavelength of 325 nm. The emission spectra of CeO_2 NPs are obtained with eight peaks at 360 nm, 375 nm, 391 nm, 411 nm, 442 nm, 452 nm, 491 nm, and 519 nm, which are shown in (Fig. 6). The spectra comprise of the three near band edge emission (360 nm, 375 nm, and 391 nm), violet emission (411 nm), two blue emissions (442 nm and 452 nm), blue-green emission (491 nm), and green emission (512 nm) for CeO_2 NPs respectively.

The NBE emission 360 nm, 375 nm, and 391 nm are attributed to a band-to-band recombination process, which possibly involving localized or free exciton (Wang *et al*. 2011). These emission peaks between 400 and 500 nm form a broad emission band. The violet emission band 411 nm is originated from the defect state existing extensively between the Ce 4f band and O 2p band (Morshed *et al*. 1997 and Lu et al. 2010). The blue emission bands (442 nm and 452 nm) can be attributed to the excitonic recombination of CeO_2 NPs (Huang *et al*. 2011 and Kim. 2001) and can be partly certificated by comparing the relationship of peak intensity and bandgap. They are due to the 5d-4f transitions of Ce^{3+} between the ^2D ($5d^1$) ground state and the $^2F_{5/2}$ (4f1) state. The blue-green emission bands (491 nm) are attributed to the transitions from different defect levels of the O 2p band. The green emission bands (512 nm) may be due to the low density of oxygen vacancies during the preparation of the CeO_2 NPs.

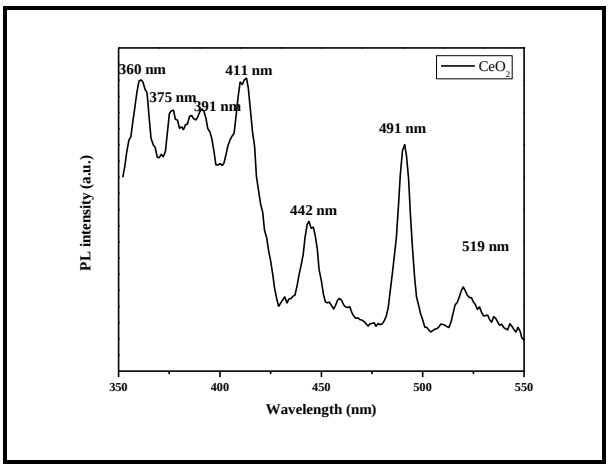

Fig. 6: Photoluminescence spectra of CeO_2 NPs.

3. CONCLUSION

The CeO_2 NPs were synthesized by the green method derived from *A. Indica* leaf extract. X-ray diffraction study confirmed that the prepared particles were of the cubic fluorite structure of CeO_2 NPs. The XPS studies showed that from the indexed peaks corresponding to Ce (3d), C (1s), and O (1s), the

respective binding energies of the elements were estimated. From the FT-Raman spectra, the sharp Raman active mode was observed at 461cm^{-1}, and this was due to the symmetrical stretching mode of the Ce-8O for CeO_2 NPs. From the TEM and FESEM images, the morphology of CeO_2 nanoparticles exhibits a spherical structure. The elemental compositions identify by EDAX spectra. In UV-Vis absorption spectra, the peak edge was observed at 314 nm for CeO_2 NPs. From the PL spectra, the low intense band edge emission peaks were obtained due to the energy released by the electrons coming down from Ce 4f level to O 2p level.

FUNDING

This research received no specific grant from any funding agency in the public, commercial, or not-for-profit sectors.

CONFLICTS OF INTEREST

The authors declare that there is no conflict of interest.

COPYRIGHT

REFERENCES

Arumugam, A., Karthikeyan, C., Haja Hameed, A. S., Gopinath, K., Gowri, S. and Karthika V., Synthesis of cerium oxide nanoparticles using *Gloriosasuperba L.* leaf extract and their structural, optical and antibacterial properties, *Mater. Sci. Eng. C.*, 49(1), 408-415(2015). https://doi.org/10.1016/j.msec.2015.01.042

Hu, J. D., Li, Y. X., Zhou, X. Z. and Cai, M. X., Preparation and characterization of ceria nanoparticles using crystalline hydrate cerium propionate as precursor, *Mater. Lett.,* 61(28), 4989-4992(2007). https://doi.org/10.1016/j.matlet.2007.03.097

Huang, Y., Cai, Y., Qiao, D. and Liu, H., Morphology-controllable synthesis and characterization of CeO_2 nanocrystals, *Particuology*, 9(2), 170-173(2011). https://doi.org/10.1016/j.partic.2010.07.023

Kim, C. G., Green emission from cerium hydroxide layers formed in Si/In/CeO_2/Si structures,*Appl. Phy. Lett.,*79(19), 3047-3049(2001). https://doi.org/10.1063/1.1416161

Liao, X. H., Zhu, J. M., Zhu, J. J. and Xu, J. Z., Chen, H.Y., Preparation of monodispersed nanocrystalline CeO_2 powders by microwave irradiation. *Chem.Commun*.,10, 937-938 (2001). https://doi.org/10.1039/b101004m

Lu, X. H., Huang, X., Xie, S. L., Zheng, D. Z., Liu, Z.Q., Liang, C.L. and Tong, Y.X., Facile electrochemical synthesis of single-crystalline CeO_2 octahedrons and their optical properties. *Langmuir*, 26(10),7569-7573 (2010). https://doi.org/10.1021/la904882t

Miki, T., Ogawa, T., Haneda, M., Kakuta, N., Ueno, A., Tateishi, S., Matsuura, S. and Sato, M., Enhanced oxygen storage capacity of cerium oxides in cerium dioxide/lanthanum sesquioxide/aluminacontaining precious metals. *J. Phys. Chem*., 94(16):6464-6467 (1990). https://doi.org/10.1021/j100379a056

Si, R., Zhang, Y. W., You, L. P. and Yan, C. H., Rare-Earth Oxide Nanopolyhedra, Nanoplates, and Nanodisks. Angew. Chem. Int. Ed.,117(21):3320-4 (2005). https://doi.org/10.1002/anie.200462573

Tsunekawa, S., Fukuda, T. and Kasuya, A., Blueshift in ultraviolet absorption spectra of monodisperse CeO_{2-x} nanoparticles. *J. Appl. Phys*., 87(3):1318-21 (2000). https://doi.org/10.1063/1.372016

Wang, Z. L. and Feng, X., Polyhedral shapes of CeO_2 nanoparticles, *J. Phys. Chem. B*., 107(49), 13563-13566 (2003). https://doi.org/10.1021/jp036815m

Wang, H., Zhu, J.J., Zhu, J.M., Liao, X.H., Xu, S., Ding, T. and Chen, H.Y., Preparation of nanocrystalline ceria particles by sonochemical and microwave-assisted heating methods. Phys. Chem. Chem. Phys., 4(15), 3794-3799(2002). https://doi.org/10.1039/b201394k

Wang, L., Ren, J., Liu, X., Lu, G. and Wang, Y., Evolution of SnO_2 nanoparticles into 3D nanoflowers through crystal growth in aqueous solution and its optical properties. *Mater.Chem.Phys*.,127(1),114-119 (2011). https://doi.org/10.1016/j.matchemphys.2011.01.043

Yao, S. Y. and Xie, Z. H., Deagglomeration treatment in the synthesis of doped-ceria nanoparticles via coprecipitation route,*J. Mater.Process. Tech.,*186(1), 54-59 (2007). https://doi.org/10.1016/j.jmatprotec.2006.12.006

Yu, T., Joo, J., Park, Y. I. and Hyeon, T., Large-Scale Nonhydrolytic Sol-Gel Synthesis of Uniform-Sized Ceria Nanocrystals with Spherical, Wire, and Tadpole Shapes. Angew. Chem., 117(45):7577-80 (2005). https://doi.org/10.1002/anie.200500992

Zhang, Y. W., Si, R., Liao, C. S., Yan, C. H., Xiao, C.X. and Kou, Y., Facile alcohothermal synthesis, size-dependent ultraviolet absorption, and enhanced CO conversion activity of ceria nanocrystals. *J.Phys. Chem. B,*107(37), 10159-67 (2003). https://doi.org/10.1021/jp034981o